Disruption of the Blood–Aqueous Barrier and Lens Abnormalities in Mice Lacking Lysyl Oxidase-Like 1 (LOXL1)

Janey L. Wiggs,[1] Basil Pawlyk,[1] Edward Connolly,[1] Michael Adamian,[1] Joan W. Miller,[1] Louis R. Pasquale,[1] Ramez I. Haddadin,[1] Cynthia L. Grosskreutz,[1] Douglas J. Rhee,[1] and Tiansen Li[1,2]

[1]Department of Ophthalmology, Harvard Medical School, Howe, Berman Gund and Angiogenesis Laboratories, Massachusetts Eye and Ear Infirmary, Boston, Massachusetts
[2]National Eye Institute, Bethesda, Maryland

Correspondence: Janey L. Wiggs, 243 Charles Street, Boston, MA 02114; janey_wiggs@meei.harvard.edu. Tiansen Li, Building 6, Room 337, 6 Center Drive, Bethesda, MD 20892; tiansen.li@nih.gov.

Submitted: August 11, 2013
Accepted: December 30, 2013

Citation: Wiggs JL, Pawlyk B, Connolly E, et al. Disruption of the blood–aqueous barrier and lens abnormalities in mice lacking lysyl oxidase-like 1 (LOXL1). *Invest Ophthalmol Vis Sci*. 2014;55:856–864. DOI:10.1167/iovs.13-13033

Purpose. Exfoliation syndrome (ES) is commonly associated with glaucoma, premature cataracts, and other ocular and systemic pathologies. *LOXL1* gene variants are significantly associated with ES; however, the role of the protein in ES development remains unclear. The purpose of this study was to characterize the ocular phenotype in *Loxl1*$^{-/-}$ (null) mice.

Methods. *Loxl1* null mice and strain-matched controls (C57BL) were evaluated by clinical and histologic analyses.

Results. Anterior segment histology showed a pronounced vesiculation of the anterior lens in the null mice. The lesions were subcapsular and in direct apposition with the posterior iris surface. Fluorescein angiography showed increased diffusion of fluorescein into the anterior chamber of the null mice compared with age-matched controls ($P = 0.003$, two-tailed, unequal variance *t*-test), suggesting compromise of the blood–aqueous barrier. Intraocular pressure measurements were within the normal range (16.5 ± 2.0 mm Hg) in null mice up to 1 year of age. Immunohistochemistry showed decreased elastin in the iris and ciliary body in the null mouse compared with controls.

Conclusions. Elimination of LOXL1 in mice impairs the blood–aqueous humor barrier in the ocular anterior segment and causes lens abnormalities consistent with cataract formation, but does not result in deposition of macromolecular material or glaucoma. These results show that mice lacking LOXL1 have some ES features but that complete disease manifestation requires other factors that could be genetic and/or environmental.

Keywords: exfoliation syndrome, LOXL1, glaucoma

Exfoliation syndrome (ES) and the related glaucoma (EG) is a common cause of blindness throughout the world.[1] Exfoliaton syndrome is characterized by the deposition of a heterogeneous mix of aggregated macromolecules throughout the ocular anterior segment, as well as in extraocular tissues.[2–4] The aggregated material is highly insoluble[5] and has a complex composition that includes plasma proteins,[6,7] extracellular matrix components,[5] and oxidative stress-induced proteins,[8] as well as lysyl oxidase-like 1 (LOXL1),[6,9] a cross-linking enzyme normally required for the formation of elastin polymer and the maintenance of elastin fibers.[10] Affected individuals also have increased elastosis in ocular tissues.[11–13] The deposition of macromolecular material is a risk factor for glaucoma causing irreversible optic nerve degeneration and blindness,[14,15] but the factors contributing to its accumulation are not fully understood. Exfoliation syndrome also predisposes to cataract formation,[3,16,17] complications during cataract surgery,[18] and possibly sensorineural hearing loss[19] and aortic aneurysm.[20] Clinical features suggesting disruption of the blood–aqueous barrier, including elevated total protein concentration in the aqueous humor of affected eyes, are well documented.[21–23]

LOXL1 was initially identified as a major genetic risk factor for ES in Nordic populations,[24] and subsequently the genetic association was confirmed in populations worldwide.[25] The risk alleles of two *LOXL1* missense changes (G153D [rs3825942] and R141L [rs1048661]) have been found in up to 98% of affected patients; however, these same variants are also found in up to 80% of unaffected individuals, suggesting that *LOXL1* abnormalities are not sufficient for disease development. Importantly, although both variants are associated with ES worldwide, the risk allele varies among different ethnic populations.[26,27] Recently in vitro studies using recombinant protein have shown that the missense variants do not affect the amine oxidase activity of LOXL1.[28] Collectively, these results show that G153D and R141L do not cause ES and that other *LOXL1* variants, possibly in linkage disequilibrium with G153D and R141L, predispose to the disease. Recent studies suggest that *LOXL1* variants influencing gene expression could underlie disease susceptibility.[29,30,31] Additionally, residence in northern latitudes is an environmental risk factor for ES,[32,33] possibly due to solar exposure and low ambient temperatures.

In previous studies of elastin homeostasis and elastogenesis, we developed a *Loxl1* null mouse and showed that LOXL1

profoundly influences the integrity of elastic fiber formation.[10] *Loxl1* null mice are unable to deposit new elastic fibers in adult tissues and accumulate soluble elastin.[34] Systemically, *Loxl1* null mice have pelvic floor dysfunction in females[34,35] and genitourinary defects in males.[36] Additionally, *Loxl1* null mice have increased choroidal neovascularization following laser induction due to abnormalities in the elastic lamina of Bruch's membrane.[37] Elastic fibers are composed of an amorphous polymer derived from tropoelastin. The covalent cross-linking of tropoelastin to form elastin requires an initial step of oxidative deamination of lysine residues catalyzed by a lysyl oxidase.[38] Among the five lysyl oxidases in the mammalian genome, LOXL1 is particularly important for elastic fiber cross-linking, and is believed to have a generalized, nonredundant role in elastic fiber homeostasis in adult tissues. To investigate the effects of decreased *LOXL1* expression on exfoliation disease development, we examined the ocular anatomy and physiology of the *Loxl1* null mouse.

Materials and Methods

Mice

Animals were housed in the Massachusetts Eye and Ear Infirmary animal facility. Animal procedures were approved by the Institutional Animal Care and Use Committee and adhered to the ARVO Statement for the Use of Animals in Ophthalmic and Vision Research. Generation of *Loxl1* null mice was previously described.[10] Briefly, targeted disruption of *Loxl1* was accomplished by deleting exon 1 and removing the translational initiation codon. Mice heterozygous or homozygous with respect to the targeted allele were identified by PCR using primers corresponding to the targeted allele. Wild-type mice were C57BL.

Intraocular Pressure Measurements

Intraocular pressure was measured in anesthetized (ketamine 100/kg and xylazine 9 mg/kg intraperitoneal) mice in a masked fashion using the rebound tonometer (TonoLab; Colonial Medical Supply, Franconia, NH). Measurements were taken between 4 and 7 minutes after anesthetic injection, done in triplicate, and then averaged.

Histology

Mouse eyes were enucleated and fixed for 10 minutes in 1% formaldehyde, 2.5% glutaraldehyde in 0.1 M cacodylate buffer (pH 7.4). Following removal of the anterior segments and lens, the eye cups were left in the same fixative at 4°C overnight. Eye cups were washed with buffer, postfixed in osmium tetroxide, dehydrated through a graded alcohol series, and embedded in Epon (Sigma-Aldrich, St. Louis, MO). Semithin sections (1 μm) were cut for light microscopy and treated with Richardson's stain (prepared as a 1:1 mixture of 1% AzureII in distilled water and 1% Methylene Blue in 1% sodium borate). For electron microscopy, ultrathin sections were stained in uranyl acetate and lead citrate before viewing on a JEOL 100CX electron microscope (JEOL Ltd., Tokyo, Japan).

Immunofluorescence

For elastin immunofluorescence staining, eyes were enucleated from *Loxl1* null and wild-type (WT) mice at 12 months of age and were fixed in 4% formaldehyde in phosphate-buffered saline (PBS) for 1 hour. The fixed tissues were then soaked in 30% sucrose–PBS overnight. On the following day the tissues were shock frozen and sectioned at 10-μm thickness in a cryostat (Leica CM1900; Leica Microsystems, Inc., Buffalo Grove, IL). Frozen sections were collected on glass slides and stained for elastin (anti-mouse α elastin, PR385 polyclonal antibody; Elastin Products Company, Owensville, MO). Sections were also counterstained with Hoechst 33342 nuclear dye (Sigma-Aldrich). Sections were examined and photographed on an Olympus IX70 inverted fluorescent microscope (Olympus America, Center Valley, PA) with a Zeiss digital camera attachment (Carl Zeiss Microscopy, Thornwood, NY).

Immunoblotting

Anterior segments from each mouse eye including iris, cornea, and ciliary bodies were dissected and extracted with 100 μL radioimmunoprecipitation assay (RIPA) buffer. After centrifugation, the pellet was discarded; and to the supernatant, an equal volume of 2× protein sample buffer (Bio-Rad, Hercules, CA) was added. After heating to 90°C for 5 minutes, the samples were run on a 10% SDS-PAGE gel and electroblotted to polyvinylidene difluoride (PVDF) membrane. After blocking, the blot was incubated with an antielastin antibody (PR385; Elastin Products Company), followed by peroxidase-conjugated secondary antibody, and developed for enhanced chemiluminescence (ECL). The blot was reprobed with a tubulin antibody for loading control.

Fluorescein Angiography and Image Analysis

Fluorescein angiography was performed by injecting 50 μL fluorescein conjugated with dextran (molecular weight [MW] 10,000) into the femoral artery and recording anterior ocular images for up to 10 minutes postinjection, using the Imagenet Digital Angiography System (Topcon TRC 50 IX retinal camera and Imagenet 2000 system; Topcon America Corp., Paramus, NJ). Ten null mice and 10 WT mice were used for this experiment, and the images captured 2 minutes after fluorescein injection were analyzed. For each image, integrated density/unit area was calculated using ImageJ (available in the public domain at http://rsbweb.nih.gov/ij/; National Institutes of Health, Bethesda, MD) and the integrated density of the limbus/unit area was compared with the integrated density/unit area of the iris without the pupil (corresponding to the anterior chamber). For each image, the ImageJ ellipse tool was used to outline, separately, (1) the entire image (limbus, pupil, and iris), (2) the iris and pupil area without the limbus, and (3) the pupil area only. For each of these three image groups, the area and the integrated density were calculated using the "measure" function. The integrated density of the iris (calculated by subtracting the pupil integrated density/area and the limbus integrated density/area from the whole eye image), corresponding to the anterior chamber space, was compared to the integrated density/area of the limbus (calculated by subtracting the iris + pupil integrated density/area from the whole eye image integrated density/area). The values of the anterior chamber integrated density/area divided by the limbus integrated density/area for the WT mice were compared with those for the null mice using two-tailed unequal variance *t*-test. A P value < 0.05 was considered statistically significant.

Postembedding Immunoelectron Microscopy

Mouse aorta were dissected and fixed in 2% formaldehyde, 0.1% glutaraldehyde in PBS for 1 hour. Fixed tissues were soaked in 30% sucrose in PBS overnight and frozen in liquid nitrogen. Thin (70 nm) sections were cut on a Leica cryo-ultramicrotome and collected on Formvar-coated nickel grids

Investigative Ophthalmology & Visual Science

(Polysciences, Inc., Warrington, PA). Grids carrying the sections were incubated with 0.15 M glycine/PBS and then blocked in 1% fish gelatin in PBS. Primary LOXL1 antibody was applied and incubated at room temperature for 2 hours. The sections were washed in Tris-buffered saline (TBS) followed by incubation with goat anti-rabbit secondary antibody conjugated to 0.8-nm gold particles, followed by silver enhancement using the AURION silver enhancement reagents (Electron Microscopy Sciences, Fort Washington, PA). Sections were poststained with 5% uranyl acetate, washed through drops of methyl cellulose, air dried, and viewed on a JEOL 100CX electron microscope.

Results

LOXL1 Deficiency Is Associated With Ocular Lens Abnormalities

On gross inspection the anterior lens of the *Loxl1* null mouse had a spotted appearance compared to the WT (Fig. 1A). The extent of the affected lens region was highly stereotypical and matched an area normally in close juxtaposition to the posterior iris epithelial lining, with relative sparing of the center region corresponding to the pupil. This phenotype was highly reproducible; in over 100 mutant lenses, we observed a 100% concordance with the *Loxl1* null genotype, and this

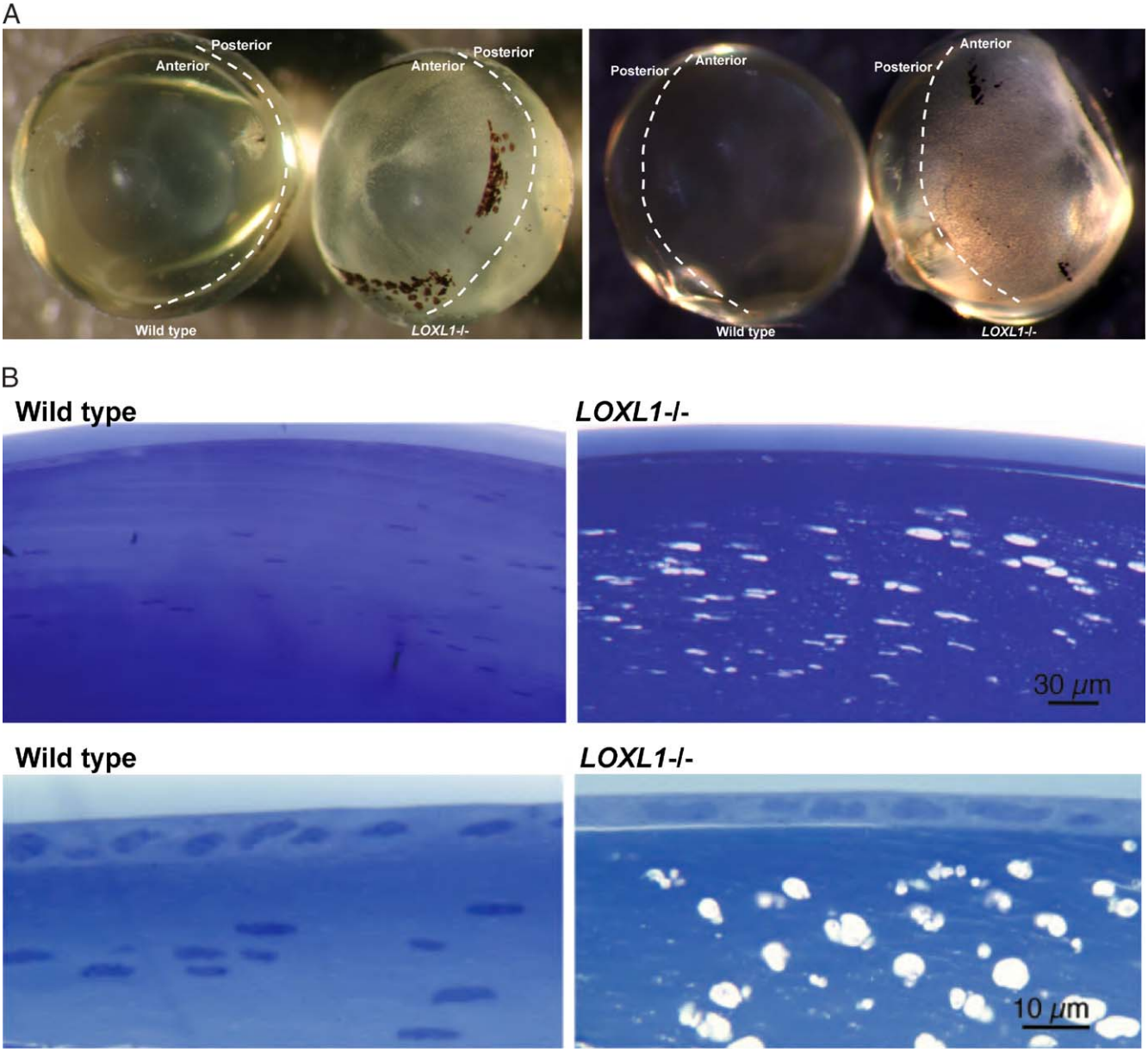

Figure 1. (**A**) Wild-type and *Loxl1*$^{-/-}$ (null) lens. Genotypes, as well as the anterior/posterior regions, are labeled. The WT lens is clear, while the *Loxl1*$^{-/-}$ lens has densely distributed white spots in the anterior aspect of the lens. The affected area corresponds to the area underlying the iris. Lenses shown are from mice at 10 months of age. Similar lens defects were observed in mice aged postnatal (P)30 days to P18 months. The *black spots* are detached pigments from the iris and are not a part of the mutant phenotype. (**B**) Light microscopy of WT (*left*) and *Loxl1*$^{-/-}$ (*right*) lens. Subcapsular vesicles are seen in the anterior cortex region of *Loxl1*$^{-/-}$ lens. The lens capsule does not show any defects in the *Loxl1*$^{-/-}$ mice. *Bottom*: higher-magnification images. (**C**) Electron microscopy of WT and *Loxl1*$^{-/-}$ mouse lens. *Top*: WT; *bottom*: *Loxl1*$^{-/-}$. In the *Loxl1*$^{-/-}$ mice the subcapsular vesicles are intracellular, and there is poor adhesion between the lens fibers and also between the lens fibers and the lens epithelium.

Investigative Ophthalmology & Visual Science

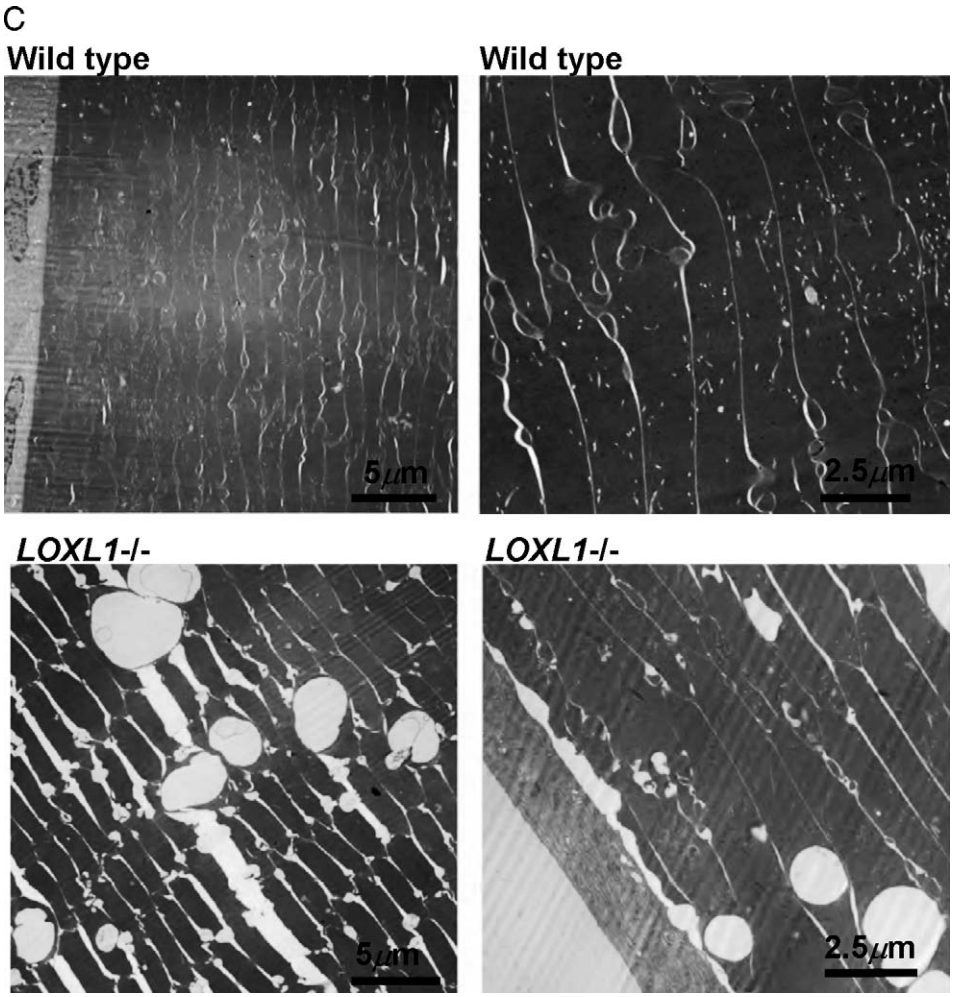

Figure 1. (**C**) Electron microscopy of WT and *Loxl1*$^{-/-}$ mouse lens. *Top*: WT; *bottom*: *Loxl1*$^{-/-}$. In the *Loxl1*$^{-/-}$ mice the subcapsular vesicles are intracellular, and there is poor adhesion between the lens fibers and also between the lens fibers and the lens epithelium.

phenotype was never seen in WT lens. These lens defects were found at all ages examined, including the youngest mice (1 month). No posterior lens opacification was present in any lens, including in mice aged up to 18 months. By light microscopy, the anterior lesions manifested as numerous vacuoles located in the subcapsular lens fibers (Fig. 1B). Electron microscopy showed that the vacuoles were intracellular and that there was increased separation between the lens fibers (Fig. 1C). The lens capsule was normal without evidence of accumulating exfoliation material, even in the oldest mice examined (18 months). The subcapsular vacuolar lens fiber defects in the null mouse are consistent with anterior subcapsular cataract formation. Lenticular vacuolar formation is the precursor to cortical and nuclear cataract in several experimental models of cataract formation.[39–41]

Fluorescein Angiography Shows Compromise of the Blood–Aqueous Barrier in *Loxl1* Null Mice

Elastin is not a known component of the ocular lens[42,43] and does not have a known function that would affect lens structure or formation. Thus the lens subcapsular vesicles likely formed through a mechanism that extrinsically, not intrinsically, compromises the lens tissue. The anterior location of the lens defects immediately posterior to the iris suggested that the lens pathology could be triggered by material coming from the iris. In human ES patients, the blood–aqueous barrier is compromised, creating abnormal accumulations of serum proteins and extracellular matrix components in the anterior chamber, as well as changes in aqueous humor pH, osmolality, and reactive oxygen species related to increased oxygen content.[21–23] We hypothesized that abnormalities in the composition of the aqueous humor in human patients,[44–46] due to compromise of the blood–aqueous barrier, could be responsible for the damage to the anterior lens observed in the null mice. To investigate this hypothesis, we evaluated the integrity of the blood–aqueous barrier in the *Loxl1* null mice by imaging the anterior ocular segment after intravascular injection of a fluorescein-dextran conjugate. Using 10 null mice and 10 age-matched WT mice (all at 8 months of age), anterior segment images captured 2 minutes after injection were analyzed to determine the relative amount of fluorescein in the anterior chamber (AC) area relative to the limbus. Using ImageJ, we measured integrated density/area for both the limbus and the region representing the AC (the iris area without the pupil) for each mouse. The integrated density/area for the AC was divided by the integrated density/area for the limbus to correct for differences in injection efficiency, eye size, and other variables affecting the total amount of fluorescein reaching the eye. The ratio of AC to limbus was higher for the null mice (mean, 0.47; range, 0.37–0.56; standard deviation, ±0.07) compared with the WT mice

Investigative Ophthalmology & Visual Science

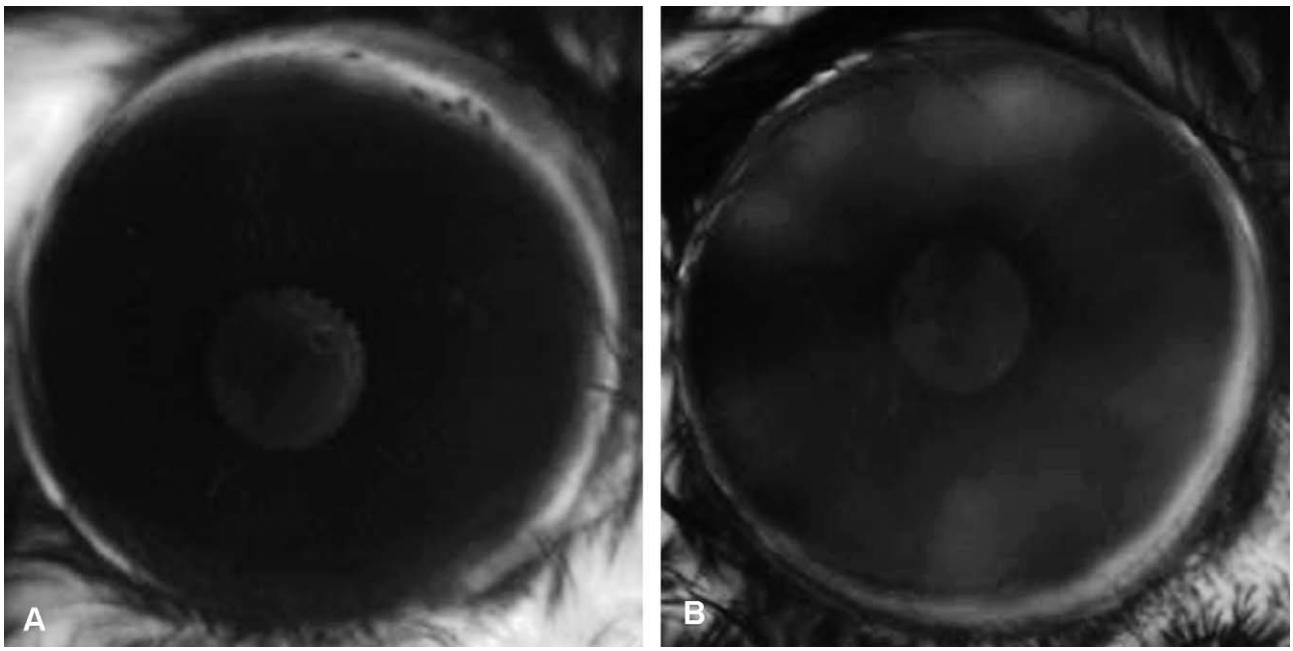

FIGURE 2. Images from anterior segment fluorescein angiograms in 8-month-old mice using fluorescein conjugated with 10K dextran at 2 minutes after injection. (**A**) WT; (**B**) *Loxl1*$^{-/-}$ (null). Increased fluorescein in the AC is evident in the *Loxl1*$^{-/-}$ mouse compared with the WT mouse. The ratio of AC to limbus integrated density is 0.41 for ([**A**]; AC integrated density/area divided by limbus integrated density/area = 31/75) and is 0.51 for ([**B**]; AC integrated density/area divided by limbus integrated density/area = 38/76).

(mean, 0.38; range, 0.28–0.46; standard deviation, ±0.04; $P = 0.003$, two-tailed unequal variance *t*-test), indicating a relative increase of conjugated fluorescein in the AC of the null mice compared with the WT (Fig. 2). These results suggest that the blood–aqueous barrier in the null mice is compromised compared to that in the WT mice.

Elastic Fibers Are Diminished in *Loxl1* Null Mouse Iris and Ciliary Body

Abnormalities in elastin formation and deposition could contribute to the compromised blood–aqueous barrier observed in the *Loxl1* null mouse. To examine elastin localization in the anterior segment structures implicated in the blood–aqueous barrier, we used immunohistochemistry to compare the staining pattern of elastin protein (tropoelastin) in the anterior segments of *Loxl1* null and WT mouse eyes (Fig. 3).

Immunofluorescence signals (yellow) for elastin in WT eyes were found to be abundant throughout the anterior segment (i.e., iris, ciliary body, and trabecular meshwork; Fig. 3A). In contrast, only background staining for elastin could be seen in the anterior segments of the null mice (Fig. 3B). A near-continuous chain of elastic fibers was observed within the stroma of WT iris (Fig. 3C) that appeared to be almost completely absent in the null iris (Fig. 3D).

Loss of LOXL1 results in an inability to deposit new elastic fibers in adult tissues that is usually associated with an increase in soluble elastin. This defect in elastic fiber homeostasis was also confirmed in the AC tissues of the mutant mouse eye as revealed by immunoblotting for elastin (Fig. 3E). Compared to the WT tissue, the mutant tissue had a prominent band at 72 kDa corresponding to the monomeric tropoelastin.

LOXL1 Protein Is Embedded With Elastin Polymers

Increased elastosis in ocular tissues, including the iris, and presence of LOXL1 in the AC are known findings in individuals with ES.[6,9,11–13] Previous studies have shown that LOXL1 immunoreactivity associates exclusively with elastic fibers[10]; however, the nature of the association is not known. To answer this question, which would help to explain the presence of LOXL1 in the AC, we performed immunoelectron microscopy for LOXL1. Although iris stroma is also rich in elastic fibers, we chose mouse aorta as the tissue for this investigation because the thickness of the elastic laminas makes it easier to observe the relationship between LOXL1 and elastin. Cross-sectional profiles of aorta show that immunogold-labeled LOXL1 is densely distributed along the amorphous elastin polymers in the WT mouse (Figs. 4A–C) but is completely absent in the *Loxl1* null mutant (Fig. 4D). The centrally distributed LOXL1 labels indicate that LOXL1 is incorporated into the elastin polymers as it forms, suggesting that as the lysine residues on tropoelastin are cross-linked, the activated substrates also spontaneously cross-link with LOXL1, making the latter a constituent of the mature elastic fibers. The exceptionally high density of the labels would empirically indicate that LOXL1 is an abundant constituent of elastic fibers, and that shedding of elastin degradation products into the aqueous humor would include relatively high amounts of LOXL1 along with other components of elastic fibers.

Absence of Aggregate Macromolecular Deposition, IOP Elevation, and Optic Nerve Degeneration in *Loxl1* Null Mice

Over 50% of patients with ES develop glaucoma associated with high IOP leading to deterioration of the optic nerve.[14,15] In the normal eye, aqueous fluid produced by the ciliary body is drained at a constant rate through the trabecular meshwork into the episcleral venous system. The accumulation of macromolecular material in the trabecular meshwork compromises this process, leading to an increase in IOP. In the null mouse, deposition of macromolecular material on ocular structures was not evident by slit-lamp exam or light microscopy. In addition, the IOP in 8-month-old null mice

Investigative Ophthalmology & Visual Science

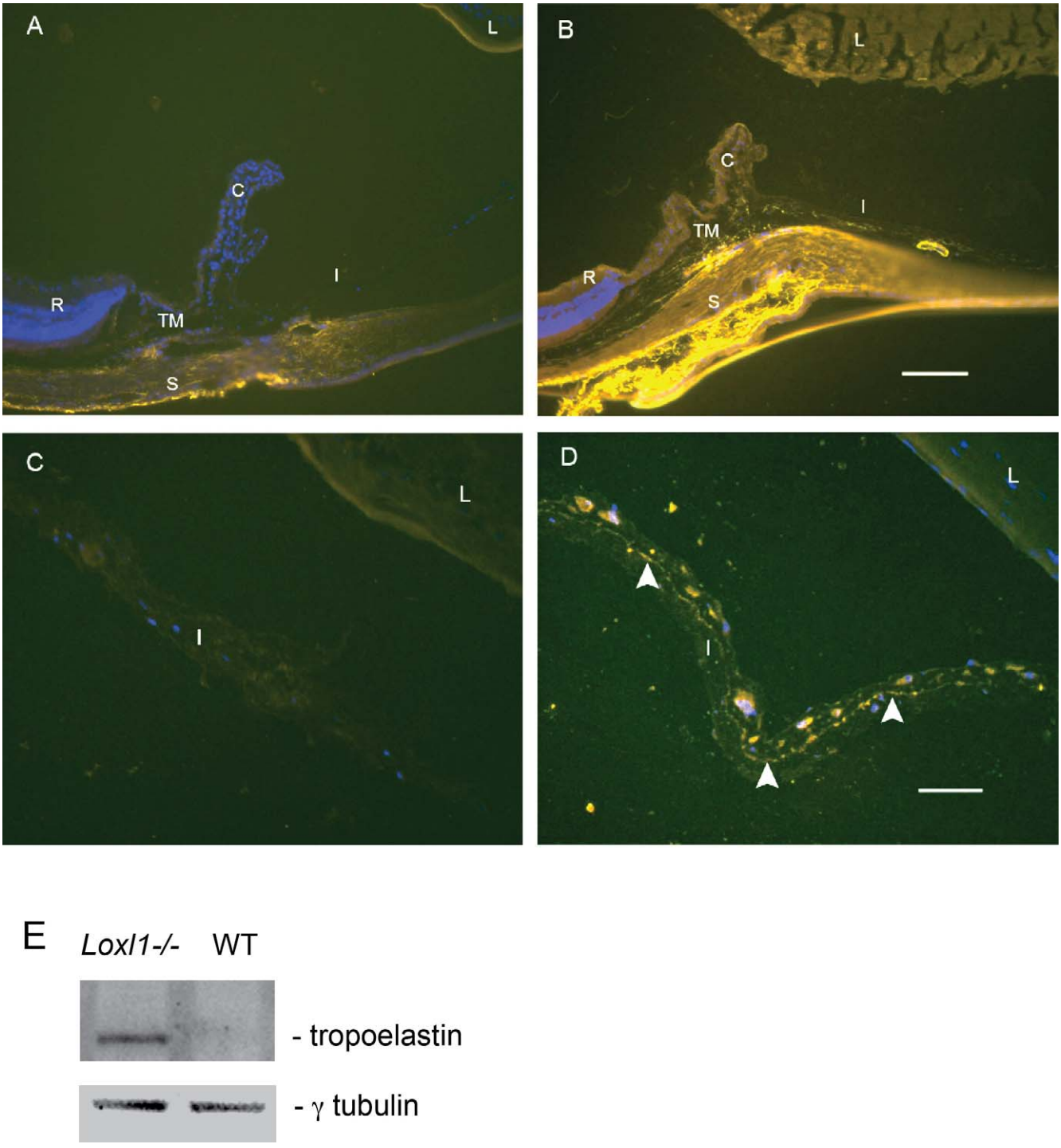

Figure 3. Immunofluorescent labeling of elastin. Immunofluorescent labeling of elastin (*yellow*) in the ocular anterior segments of a *Loxl1* null mouse (**A**) and an age-matched WT mouse (**B**). Higher magnification (40×) of the iris from the *Loxl1* null (**C**) and WT mouse (**D**). *White arrowheads* point to the near-continuous chain of elastin fibers in the WT iris. Cell nuclei labeled with Hoechst dye appear *blue*. (**A**, **B**) *Scale Bar*: 100 μm. (**C**, **D**) *Scale Bar*: 50 μm. C, ciliary body; I, iris; L, lens; R, retina; S, sclera; TM, trabecular meshwork. (**E**) Soluble elastin accumulates in the mutant AC tissues as shown by the band corresponding to tropoelastin.

was not significantly elevated (null: 16.6 ± 2.2 mm Hg (n = 12); WT: 16.7 ± 1.0 mm Hg (n = 8); P = 0.89) or in mice aged up to 2 years (null: 15.6 ± 2.5 mm Hg (n = 12); WT: 16.6 ± 2.7 mm Hg (n = 12); P = 0.33). Consistent with normal ocular pressure, the *Loxl1* null mice, even those aged up to 1 year, did not show significant ganglion cell loss or other pathology of the optic nerve (data not shown).

Discussion

We have documented phenotype changes in the murine eye associated with loss of LOXL1 function that resemble some aspects of human ES. We have shown that *Loxl1* null mice have defects in the anterior lens consistent with subcapsular cataract formation in regions proximal to overlying iris, and

Investigative Ophthalmology & Visual Science

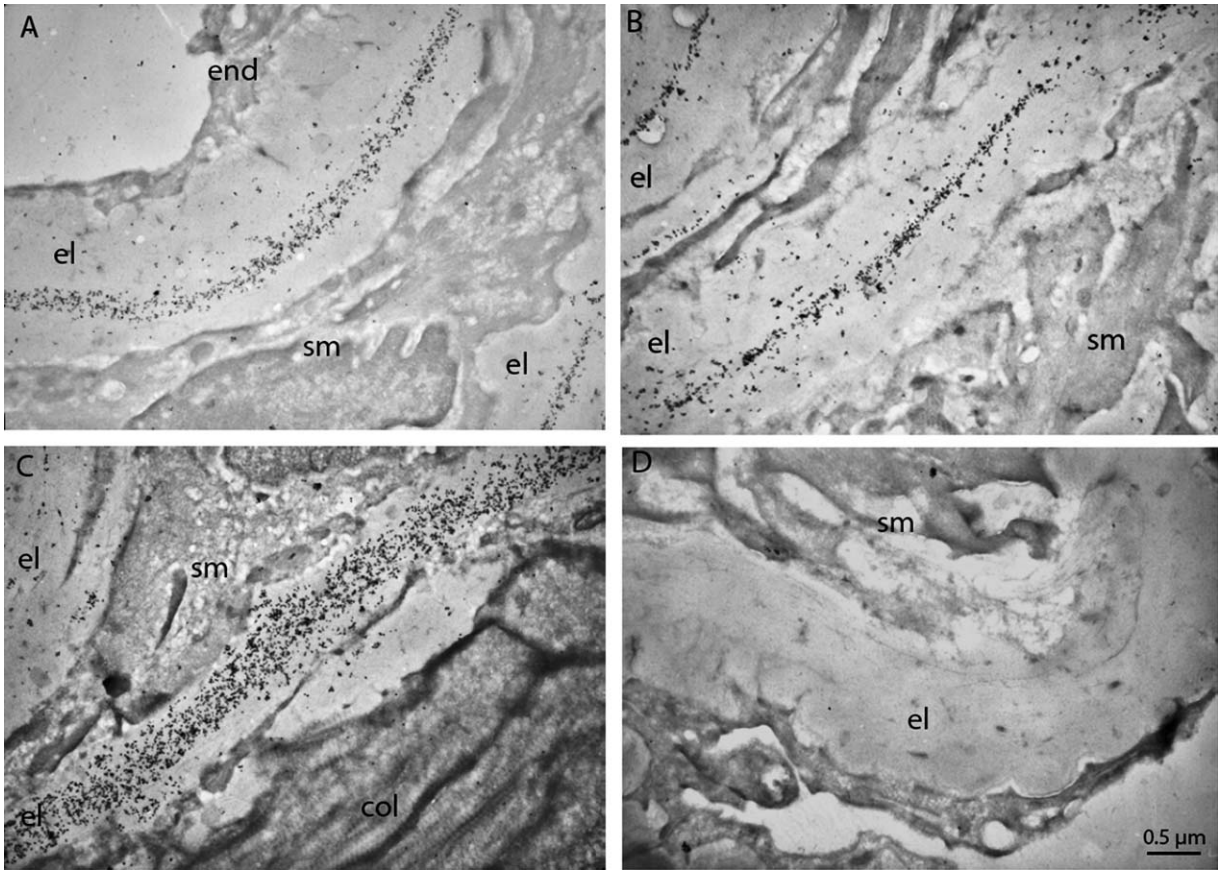

Figure 4. Ultrastructural localization of LOXL1 in the aorta. LOXL1 is associated exclusively with the elastic laminas in the aortas of the WT mice (**A–C**). LOXL1 shows a tendency to be located in the core rather than the mantle layer of the elastic laminas. Aorta of a *Loxl1*$^{-/-}$ mouse (**D**) was devoid of any LOXL1 immunostaining. *Scale Bar*: 0.5 μm; el, elastic lamina; col, collagen fibers; end, endothelium; sm, smooth muscle cells.

that the blood–aqueous barrier of the mutant mice is compromised. These results could suggest that loss of LOXL1 predisposes to cataract formation through a mechanism involving leakage of macromolecular components from blood circulation. While the degree of blood–aqueous compromise in mice, and subsequent lens damage, could be different from what is seen in humans and other primates, exfoliation patients do have an increased risk of cataract.[3,16,17] In the Blue Mountains Eye Study, patients with ES had a nearly 2-fold increase in cataract risk compared to individuals without ES (odds ratio [OR], 1.90; 95% confidence interval [CI], 1.04–3.48).[16] Our results suggest that cataract formation in exfoliation patients and in *Loxl1* null mice could be secondary to compromise of the blood–aqueous barrier caused by LOXL1 insufficiency. Our results also show diminished elastic fibers in the *Loxl1* null iris compared to the WT iris and identify LOXL1 as a constituent of elastin fibers, suggesting that elastosis, another documented feature of ES in humans,[11–13] would release soluble elastin-derived peptides, including LOXL1, into the aqueous humor in affected patients. The location of the lens defects proximal to the iris suggests that these soluble peptides could contribute to the resulting lens abnormalities. Although further experimentation will be necessary to identify the agent(s) responsible for lens damage, this information could have significant relevance to the future development of novel preventive therapies.

The *Loxl1* null mice do not exhibit spontaneous accumulation of exfoliation material characteristic of human ES. These findings are consistent with current genetic data suggesting that additional genetic and/or environment factors aside from genetic variation in *LOXL1* are necessary for disease development.[24–27,32,33] Thus while a constitutive loss of LOXL1 clearly partially replicates the pathophysiology of ES, it is not sufficient to produce the full disease spectrum, at least not in mice.

The deposition of aggregated macromolecular material on ocular structures is correlated with elevated IOP and subsequent optic nerve disease in human exfoliation glaucoma patients.[14,15] The absence of this material in the *Loxl1* null mouse eyes is consistent with normal ocular pressure and normal optic nerves. As LOXL1 is a component of the aggregated macromolecular material,[6,9] its activity may be required for the formation of macromolecular aggregates. In humans the aggregated material is resistant to solubilization, even under harsh conditions, suggesting that covalent bonds are present in the deposited material.[5] Since LOXL1 is an abundant component of the elastic fibers, elastosis would be expected to cause LOXL1 to leak into the AC where it may catalyze cross-linking of serum proteins also leaked into the AC. Thus both LOXL1 and a compromised blood–aqueous barrier could be required for producing macromolecular deposition and glaucoma. Paradoxically, while this study suggests that functional insufficiency of LOXL1 plays a role in the pathogenesis of ES, complete ablation of LOXL1 in the null mouse may have precluded protein cross-linking and aggregate formation. This view appears consistent with the observation that a decline in *LOXL1* expression precedes disease progression.[30,31] Further studies, perhaps employing a combination of environmental factors such as solar exposure and low temperature (which may increase elastosis or interfere with

elastin polymer formation by blocking coacervation) and genetic manipulation of *LOXL1* (other than null), may lead to an animal model that fully replicates the human disease. Such a model could further define the underlying disease mechanism, making it possible to design and test therapies.

Acknowledgments

We thank Frederick Jakobiec for assistance with the lens pathology. We thank Juliet Xu for technical assistance.

Supported by National Institutes of Health Grants R21EY019161 (TL), R01EY020928 (JLW), and P30EY014104; Research to Prevent Blindness; the Massachusetts Lions Eye Research Fund; the Harvard Glaucoma Center of Excellence; and a Distinguished Ophthalmology Scholar award (LRP). The authors alone are responsible for the content and writing of the paper.

Disclosure: **J.L. Wiggs**, None; **B. Pawlyk**, None; **E. Connolly**, None; **M. Adamian**, None; **J.W. Miller**, None; **L.R. Pasquale**, None; **R.I. Haddadin**, None; **C.L. Grosskreutz**, None; **D.J. Rhee**, None; **T. Li**, None

References

1. Vesti E, Kivela T. Exfoliation syndrome and exfoliation glaucoma. *Prog Retin Eye Res*. 2000;19:345–368.
2. Schlotzer-Schrehardt U. Molecular pathology of pseudoexfoliation syndrome/glaucoma–new insights from LOXL1 gene associations. *Exp Eye Res*. 2009;88:776–785.
3. Schlotzer-Schrehardt U, Naumann GO. Ocular and systemic pseudoexfoliation syndrome. *Am J Ophthalmol*. 2006;141: 921–937.
4. Streeten BW, Li ZY, Wallace RN, Eagle RC, Keshgegian AA. Pseudoexfoliative fibrillopathy in visceral organs of a patient with pseudoexfoliation syndrome. *Arch Ophthalmol*. 1992; 110:1757–1762.
5. Ovodenko B, Rostagno A, Neubert TA, et al. Proteomic analysis of exfoliation deposits. *Invest Ophthalmol Vis Sci*. 2007;48: 1447–1457.
6. Creasey R, Sharma S, Gibson CT, et al. Atomic force microscopy-based antibody recognition imaging of proteins in the pathological deposits in pseudoexfoliation syndrome. *Ultramicroscopy*. 2011;111:1055–1061.
7. Lee RK. The molecular pathophysiology of pseudoexfoliation glaucoma. *Curr Opin Ophthalmol*. 2008;19:95–101.
8. Gartaganis SP, Patsoukis NE, Nikolopoulos DK, Georgiou CD. Evidence for oxidative stress in lens epithelial cells in pseudoexfoliation syndrome. *Eye*. 2007;21:1406–1411.
9. Sharma S, Chataway T, Burdon KP, et al. Identification of LOXL1 protein and apolipoprotein E as components of surgically isolated pseudoexfoliation material by direct mass spectrometry. *Exp Eye Res*. 2009;89:479–485.
10. Liu X, Zhao Y, Gao J, et al. Elastic fiber homeostasis requires lysyl oxidase-like 1 protein. *Nat Genet*. 2004;36:178–182.
11. Netland PA, Ye H, Streeten BW, Hernandez MR. Elastosis of the lamina cribrosa in pseudoexfoliation syndrome with glaucoma. *Ophthalmology*. 1995;102:878–886.
12. Pena JD, Netland PA, Vidal I, Dorr DA, Rasky A, Hernandez MR. Elastosis of the lamina cribrosa in glaucomatous optic neuropathy. *Exp Eye Res*. 1998. 67:517–524.
13. Streeten BW, Bookman L, Ritch R, Prince AM, Dark AJ. Pseudoexfoliative fibrillopathy in the conjunctiva. A relation to elastic fibers and elastosis. *Ophthalmology*. 1987;94:1439–1449.
14. Ekström C, Alm A. Pseudoexfoliation as a risk factor for prevalent open-angle glaucoma. *Acta Ophthalmol*. 2008;86: 741–746.
15. Ritch R. The management of exfoliative glaucoma. *Prog Brain Res*. 2008;173:211–224.
16. Kanthan GL, Mitchell P, Burlutsky G, Rochtchina E, Wang JJ. Pseudoexfoliation syndrome and the long-term incidence of cataract and cataract surgery: the Blue Mountains Eye Study. *Am J Ophthalmol*. 2013;155:83–88.
17. Summanen P, Tonjum AM. Exfoliation syndrome among Saudis. *Acta Ophthalmol*. 1988;184:107–111.
18. Shingleton BJ, Marvin AC, Heier JS, et al. Pseudoexfoliation: high risk factors for zonule weakness and concurrent vitrectomy during phacoemulsification. *J Cataract Refract Surg*. 2010;36:1261–1269.
19. Yazdani S, Tousi A, Pakravan M, Faghihi AR. Sensorineural hearing loss in pseudoexfoliation syndrome. *Ophthalmology*. 2008;115:425–429.
20. Schumacher S, Schlotzer-Schrehardt U, Martus P, Lang W, Naumann GO. Pseudoexfoliation syndrome and aneurysms of the abdominal aorta. *Lancet*. 2001;357:359–360.
21. Kuchle M, Vinores SA, Mahlow J, Green WR. Blood-aqueous barrier in pseudoexfoliation syndrome: evaluation by immunohistochemical staining of endogenous albumin. *Graefes Arch Clin Exp Ophthalmol*. 1996;234:12–18.
22. Schumacher S, Nguyen NX, Kuchle M, Naumann GO. Quantification of aqueous flare after phacoemulsification with intraocular lens implantation in eyes with pseudoexfoliation syndrome. *Arch Ophthalmol*. 1999;117:733–735.
23. Wang L, Yamasita R, Hommura S. Corneal endothelial changes and aqueous flare intensity in pseudoexfoliation syndrome. *Ophthalmologica*. 1999;213:387–391.
24. Thorleifsson G, Magnusson KP, Sulem P, et al. Common sequence variants in the LOXL1 gene confer susceptibility to exfoliation glaucoma. *Science*. 2007;317:1397–1400.
25. Fan BJ, Wiggs JL. Glaucoma: genes, phenotypes, and new directions for therapy. *J Clin Invest*. 2010;120:3064–3072.
26. Ozaki M, Lee KY, Vithana EN, et al. Association of LOXL1 gene polymorphisms with pseudoexfoliation in the Japanese. *Invest Ophthalmol Vis Sci*. 2008;49:3976–3980.
27. Williams SE, Whigham BT, Liu Y, et al. Major LOXL1 risk allele is reversed in exfoliation glaucoma in a black South African population. *Mol Vis*. 2010;16:705–712.
28. Kim S, Kim Y. Variations in LOXL1 associated with exfoliation glaucoma do not affect amine oxidase activity. *Mol Vis*. 2012; 18:265–270.
29. Fan BJ, Pasquale LR, Rhee D, Li T, Haines JL, Wiggs JL. LOXL1 promoter haplotypes are associated with exfoliation syndrome in a U.S. Caucasian population. *Invest Ophthalmol Vis Sci*. 2011;52:2372–2378.
30. Schlötzer-Schrehardt U, Pasutto F, Sommer P, et al. Genotype-correlated expression of lysyl oxidase-like 1 in ocular tissues of patients with pseudoexfoliation syndrome/glaucoma and normal patients. *Am J Pathol*. 2008;173:1724–1735.
31. Zenkel M, Krysta A, Pasutto F, Juenemann A, Kruse FE, Schlötzer-Schrehardt U. Regulation of lysyl oxidase-like 1 (LOXL1) and elastin-related genes by pathogenic factors associated with pseudoexfoliation syndrome. *Invest Ophthalmol Vis Sci*. 2011;52:8488–8495.
32. Kang JH, Loomis S, Wiggs JL, Stein JD, Pasquale LR. Demographic and geographic features of exfoliation glaucoma in 2 United States-based prospective cohorts. *Ophthalmology*. 2012;119:27–35.
33. Stein JD, Pasquale LR, Talwar N, et al. Geographic and climatic factors associated with exfoliation syndrome. *Arch Ophthalmol*. 2011;129:1053–1060.
34. Liu X, Zhao Y, Pawlyk B, Damaser M, Li T. Failure of elastic fiber homeostasis leads to pelvic floor disorders. *Am J Pathol*. 2006;168:519–528.

35. Lee UJ, Gustilo-Ashby AM, Daneshgari F, et al. Lower urogenital tract anatomical and functional phenotype in lysyl oxidase like-1 knockout mice resembles female pelvic floor dysfunction in humans. *Am J Physiol Renal Physiol*. 2008;295:545–555.
36. Wood HM, Lee UJ, Vurbic D, et al. Sexual development and fertility of Loxl1-/- male mice. *J Androl*. 2009;30:452–459.
37. Yu HG, Liu X, Kiss S, et al. Increased choroidal neovascularization following laser induction in mice lacking lysyl oxidase-like 1. *Invest Ophthalmol Vis Sci*. 2008;49:2599–2605.
38. Kagan HM, Li W. Lysyl oxidase: properties, specificity, and biological roles inside and outside of the cell. *J Cell Biochem*. 2003;88:660–672.
39. Sasaki K, Kuriyama H, Yeh LI, Fukuda M. Studies on diabetic cataract in rats induced by streptozotocin. I. Photodocumentation of lens opacification. *Ophthalmic Res*. 1983;15:185–190.
40. Hoyer HE. The effect of calcium on the lens ultrastructure. *Graefes Arch Clin Exp Ophthalmol*. 1985;223:169–173.
41. Shearer TR, Anderson RS. Histologic changes during selenite cataractogenesis: a light microscopy study. *Exp Eye Res*. 1985; 40:557–565.
42. Wang-Su ST, McCormack AL, Yang S, et al. Proteome analysis of lens epithelia, fibers, and the HLE B-3 cell line. *Invest Ophthalmol Vis Sci*. 2003;44:4829–4836.
43. Gelman S, Cone FE, Pease ME, Nguyen TD, Myers K, Quigley HA. The presence and distribution of elastin in the posterior and retrobulbar regions of the mouse eye. *Exp Eye Res*. 2010; 90:210–215.
44. Yagci R, Ersoz I, Erdurmus M, Gurel A, Duman S. Protein carbonyl levels in the aqueous humour and serum of patients with pseudoexfoliation syndrome. *Eye*. 2008;22:128–131.
45. Gartaganis SP, Georgakopoulos CD, Patsoukis NE, Gotsis SS, Gartaganis VS, Georgiou CD. 2005. Glutathione and lipid peroxide changes in pseudoexfoliation syndrome. *Curr Eye Res*. 2005;30:647–651.
46. Bleich S, Roedl J, Von Ahsen N, et al. Elevated homocysteine levels in aqueous humor of patients with pseudoexfoliation glaucoma. *Am J Ophthalmol*. 2004;138:162–164.

Investigative Ophthalmology & Visual Science